Transformer-Based Dual-Mode VCO for Multi-Mode Multi-Standard Receiver

Xiangning Fan, Xiaoyang Shi, and Li Tang

Institute of RF&OE-ICs, School of Information Science and Engineering
Southeast University, Nanjing, 210096, China
xnfan@seu.edu.cn

Abstract ─ The proposed VCO in this paper is used for multi-mode multi-standard wireless transceiver. The overall scheme includes two VCOs, each VCO adopts transformer-based structure. On-chip transformer which uses coplanar central tap structure and adopts the top metal winding is present. The primary and secondary inductances adopt octagon differential structure. Electromagnetic field (EM) simulation is carried out by using ADS Momentum. Negative conductance unit adopts the current reuse of cross coupled MOSFET. Oscillation mode can be chosen by switch. The primary and secondary inductances of the transformer are connected with 4 bit binary switches capacitor arrays and varactors under different oscillation modes to extend the range of frequency adjustment. Measurement results show that the frequency range is from 1.2 to 7.3 GHz and the phase noise at 1 MHz offset is less than -80 dBc/Hz in the whole frequency range.

Index Terms ─ Dual-mode VCO, transformer, wideband.

I. INTRODUCTION

The ever-increasing demand for the wide range wireless services is continuously generating new standards, which often come with new frequency bands or new modulation schemes [1-5]. Wireless receivers capable for supporting multi-mode multi-standard applications are highly desirable, and have become a hot spot. Phase-locked loop (PLL), as one of the most critical building blocks in RF front-end, is widely used in wireless systems. As the core of the PLL, the voltage-controlled oscillator (VCO), together with frequency-extension circuits, should be continuously tunable within a wide frequency range to fulfill the requirement of the ubiquitous connectivity and the new emerging standards. It is one of the main bottlenecks of achieving fully integrated multi-mode multi-standard receivers.

Owing to the low phase noise performance, LC-VCOs are preferred rather than ring oscillators, but their frequency range is limited owing to the low C_{max}/C_{min} ratio of the varactor. To widen the frequency range, most LC-VCOs use switched capacitors [6] or inductors [7].

However, these approaches suffer from the channel resistance and parasitic capacitance of the switch, which tend to degrade the phase noise performance and frequency tuning range. Recently, a transformer-based resonator that is able to generate two distinct frequency bands was exploited to realize dual-band VCOs or wideband VCOs [8]. In this paper, we propose a new transformer-based VCO that adopts a current-reused configuration, and apply it to the multi-mode multi-standard wireless receivers.

The rest of this paper is organized as follows. Circuit architecture and transformer design are shown in Section II. Measurement results are given in Section III, with the conclusion in Section IV.

II. CIRCUIT ARCHITECTURE AND TRANSFORMER DESIGN

Multi-mode multi-standard wireless applications need a larger frequency range, but it can typically not be achieved in traditional resonant tanks with a sufficient quality factor and phase-noise. In principle, we use two VCOs (VCOH and VCOL) to achieve the whole frequency range, and each VCO adopts transformer-based structure.

A. Oscillation frequency

Figure 1 (a) shows the general model of the one-port dual-band oscillator. Resistive components are added in series with the inductors and capacitors to account for the loss of the network, which can be typically compensated for oscillation by employing a negative transconductance cell at Port-1 or Port-2. The component Qs are defined as $Q_{L1}=\omega L_1/R_{L1}$, $Q_{C1}=1/(\omega C_1 R_{C1})$, $Q_{L2}=\omega L_2/R_{L2}$, and $Q_{C2}=1/(\omega C_2 R_{C2})$.

To facilitate the calculation of the tank impedance, the transformer is replaced by an equivalent network as shown in Fig. 1 (b), and the impedance Z_{L1} can be derived as (1)-(3), where Z_{L1} contains an equivalent inductor L_1 in series with a resistor ΔR_{L1}, and the angle frequencies ω_1 and ω_2 are given by $\omega_1 = 1/\sqrt{L_1 C_1}$, and $\omega_2 = 1/\sqrt{L_2 C_2}$:

$$Z_{L1} = \Delta R_{L1} + j\omega L_1', \tag{1}$$

$$\Delta R_{L1} = \frac{\frac{L_1}{k^2 L_2}(R_{L2} + R_{C2})(\omega L_1)^2}{[\frac{L_1}{k^2 L_2}(R_{L2} + R_{C2})]^2 + (\frac{\omega L_1}{k^2})^2 [1 - (\frac{\omega_2}{\omega})^2]^2}, \tag{2}$$

$$L_1' = \frac{[\frac{L_1}{k^2 L_2}(R_{L2} + R_{C2})]^2 + (\frac{\omega L_1}{k^2})^2 [1 - (\frac{\omega_2}{w})^2][1 - k^2 - (\frac{\omega_2}{\omega})^2]}{[\frac{L_1}{k^2 L_2}(R_{L2} + R_{C2})]^2 + (\frac{\omega L_1}{k^2})^2 [1 - (\frac{\omega_2}{\omega})^2]^2} L_1. \tag{3}$$

(a)

(b)
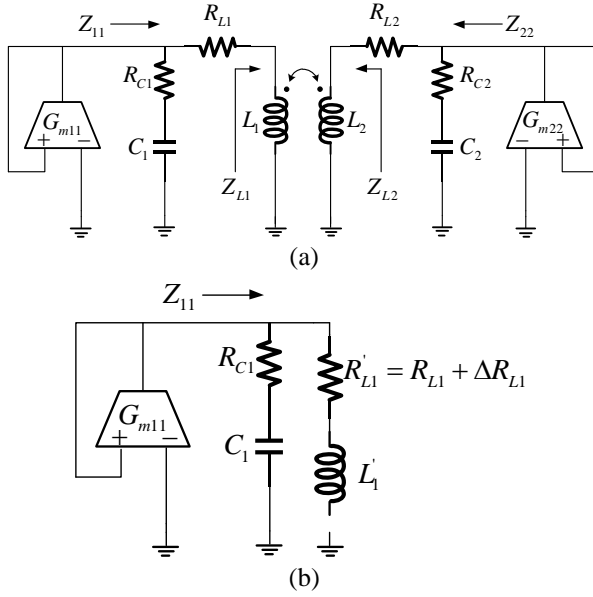
Fig. 1. Models of one port oscillators: (a) general model, and (b) simplified network for Z11 calculation.

Without loss of generality, let's define $L_1 = mL_2 = mL$, $C_1 = nC_2 = nC$ and assume in all the following discussions that $k > 0$ and $mn > 1$, so that $\omega_1 < \omega_2$. Z_{11} can be considered as a simplified LC tank as shown in Fig. 1 (b). The frequency response of Z_{11} can be quickly estimated by assuming a low-loss case, in which case Z_{11} can be derived as:

$$Z_{11} \approx (1/sC_1) \| (sL_1') = \frac{j\omega_1^2 L_1 \omega[(1-k^2)\omega^2 - \omega_2^2]}{(k^2 - 1)\omega^4 + (\omega_1^2 + \omega_2^2)\omega^2 - \omega_1^2 \omega_2^2}. \tag{4}$$

Because of the symmetry of the network in Fig. 1 (a), Z_{22} can be directly rewritten from Z_{11} as:

$$Z_{22} = \frac{j\omega_2^2 L_2 \omega[(1-k^2)\omega^2 - \omega_1^2]}{(k^2 - 1)\omega^4 + (\omega_1^2 + \omega_2^2)\omega^2 - \omega_1^2 \omega_2^2}. \tag{5}$$

From (4) and (5), Z_{11} and Z_{22} have exactly the same two peak frequency located at:

$$\omega_{H/L}^2 = \frac{\omega_1^2 + \omega_2^2 \pm \sqrt{(\omega_1^2 - \omega_2^2)^2 + 4k^2 \omega_1^2 \omega_2^2}}{2(1 - k^2)}. \tag{6}$$

Besides the zero frequency, there is only one notch frequency $\omega_{1,notch}$ in Z_{11}, and similarly, there exits only one notch frequency $\omega_{2,notch}$ in Z_{22}, which are given by:

$$\omega_{1,notch} = \frac{\omega_1}{\sqrt{1 - k^2}}, \tag{7}$$

$$\omega_{2,notch} = \frac{\omega_2}{\sqrt{1 - k^2}}. \tag{8}$$

B. Start up conditions

Figure 2 (a) and Fig. 2 (b) plot the magnitude and phase response of Z_{11} and Z_{22} with high-Q components. The phase shift begins from 90° at low frequency, cross 0° at the first peak frequency, returns to 90 after either $\omega_{1,notch}$ in Z_{11} or $\omega_{2,notch}$ in Z_{22}, and cross 0° again at the second peak frequency.
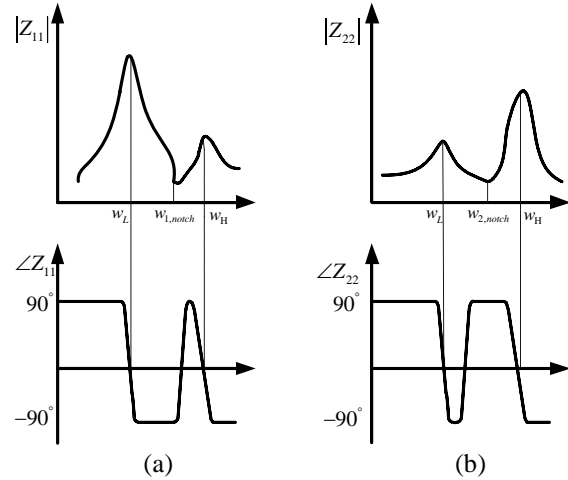

(a)   (b)

Fig. 2. Frequency response of the fourth-order LC tank of: (a) Z_{11} and (b) Z_{22}.

The start-up conditions of the one-port oscillator shown in Fig. 1 (a) are given by:

$$G_{m11} > \frac{1}{real\{Z_{11}\}}, \tag{9}$$

$$imag\{Z_{11} = 0\}. \tag{10}$$

If the tank Q is high enough, from (9), the minimum G_m for oscillation can be expressed as:

$$G_{m11,min} = \frac{(R_{L1}' + R_{C1})C_1}{L_1'}. \tag{11}$$

Putting (2) and (3) into (11), it can be derived that:

$$G_{m11,\min} = \frac{1}{A_1 \omega_{osc} L_1}[\frac{1}{A_1}\frac{1}{Q_{L1}} + \frac{1}{Q_{C1}} + \lambda(\frac{1}{A_2}\frac{1}{Q_{L2}} + \frac{1}{Q_{C2}})], \quad (12)$$

where $A_1 = \omega_1^2/\omega_{osc}^2$, $A_2 = \omega_2^2/\omega_{osc}^2$, and $\lambda = (A_2(A_1-1))/(A_1(A_2-1))$.

Symmetrically, $G_{m22,\min}$ can be easily rewritten from (12) as:

$$G_{m22,\min} = \frac{1}{A_2 \omega_{osc} L_2}[\frac{1}{A_2}\frac{1}{Q_{L2}} + \frac{1}{Q_{C2}} + \lambda^{-1}(\frac{1}{A_1}\frac{1}{Q_{L1}} + \frac{1}{Q_{C1}})].$$
$$(13)$$

At both the potential oscillation frequencies ω_L and ω_H, the phase shift is 0°, and thus (10) is satisfied, and the necessary and sufficient conditions for start-up oscillation at ω_L or ω_H would become $G_{m11} > G_{m11,\min}(\omega_L)$ or $G_{m11} > G_{m11,\min}(\omega_H)$, respectively. If G_{m11} is large enough to satisfy the two conditions, the oscillator can potentially oscillator at either frequency ω_L or ω_H or concurrently oscillator at both frequencies. The final steady-state oscillation depends on detailed configuration of the high-order LC tank and specific form nonlinearity of the active device [9].

In general, $|k| \to 0$ is undesirable in terms of the chip area as the two coils of the transformer need to be completely decoupled from each other. It would be more desirable to make $mn \to \infty$, which is equivalent to $\omega_2 \gg \omega_1$. With different value of ω_2/ω_1 and k, the transconductance ratio is always larger than 1, which implies that if the cross-coupled G_m cell placed Port 1 to compensate the loss of the tank, the VCO always prefers to oscillator at the lower peak frequency ω_L. Moreover, the larger the ratio ω_2/ω_1 is, the more stable the oscillation becomes. In order to enable stable oscillation at ω_H, the oscillator can be designed such that $G_{m22,\min}(\omega_H) < G_{m22} < G_{m22,\min}(\omega_L)$. In this case, the values of $\sqrt{mn}$ and k need to be properly chosen.

Figure 3 gives out the architecture of the proposed VCO. It consists of a transformer-based resonator and two switched differential transistor pairs. The resonator includes two identical LC tanks coupled by the transformer, and has two resonator frequencies.

The two differential pairs (MN1, MP1 and MN2, MP2) can be switched to simulate a desired oscillation mode and damps the other. When switches SW_L (SW_H) are turned on and SW_H (SW_L) are turned off, the cross-coupled transistors MN1(MN2) and MP1(MP2) generate negative resistance to compensate the loss of the transformer-based resonator. Thus, the VCO operates as a two-port oscillators at low (high) band ω_L (ω_H). Since

no lossy switches are added to the resonator, it does not degrade the phase noise performance while mode switching. In each mode, switched capacitor arrays which are controlled by 4-bit digital control code, and varactors which are tuned by V_T, are adopted for coarse and fine tuning, respectively. Note that, each differential pair is constructed by series stacking of an NMOS and a PMOS. This solution offers three advantages. First, the current consumption can be reduced by half with respect to the traditional VCOs while providing the same negative resistance [10]. Secondly, it is inherently immune to the phase noise degradation caused by second-harmonic terms since no common-source node exists. Thirdly, less transistors connected to the resonator means low parasitic capacitance, which is beneficial to the frequency tuning range.
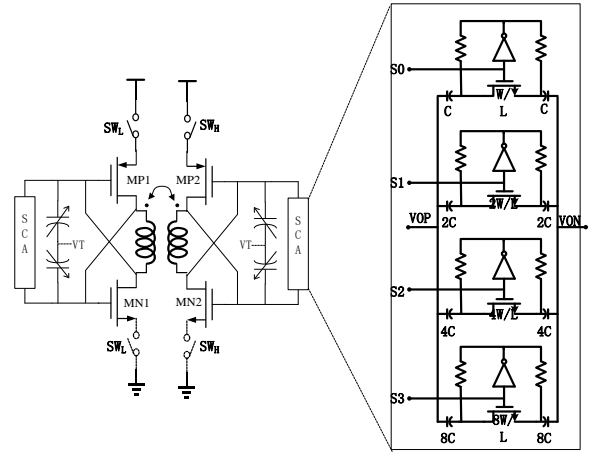

Fig. 3. Schematic of the proposed VCOs: VCOH and VCOL.

A major challenge is the implementation of the transformer. In the design of the transformer, two issues have to be addressed: (1) two ports should be on the same side to facilitate connection with capacitors; (2) two coils are weakly coupled. To achieve these goals, we design the transformers as shown in Fig. 4. The geometry size of the transformer used in VCOH in Fig. 4 (a) is shown below: two-turn primary coil has an inner radius of 125μm, the width and spacing is 18μm and 4μm, two-turn secondary coil has an inner radius of 65μm, the width and spacing is 12μm and 4μm, each coil is placed in a common-centric configuration and is implemented using the top thick mental6 layer (2.34μm) in the used technology. Electromagnetic simulation results using ADS Momentum are shown in Fig. 5. The geometry size of the transformer used in VCOL in Fig. 4 (b) is shown below: two-turn primary coil has an inner radius of 250μm, the width and spacing is 28μm and 4μm, two-turn secondary coil has an inner radius of 125μm, the

width and spacing is 28μm and 4μm, each coil is placed in a common-centric configuration and is implemented using the top thick mental6 layer (2.34μm) in the used technology. Electromagnetic simulation results using ADS Momentum are shown in Fig. 6.

As the simulation result shows, the coupling coefficient is small enough to ensure the two coils of the transformer is weakly coupled. The quality factor Q is high enough in the working band of the VCO.
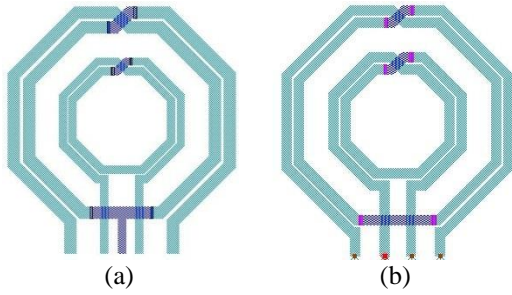

Fig. 4. Transformer layout: (a) transformer in VCOH, and (b) transformer in VCOL.
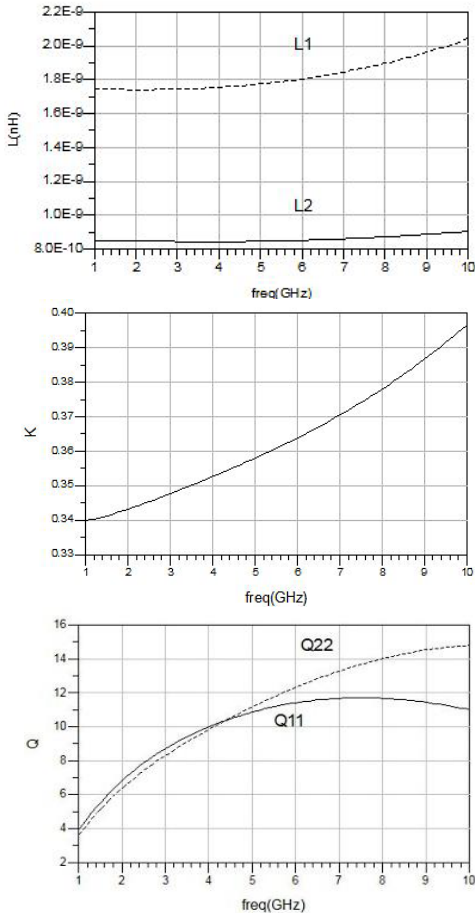

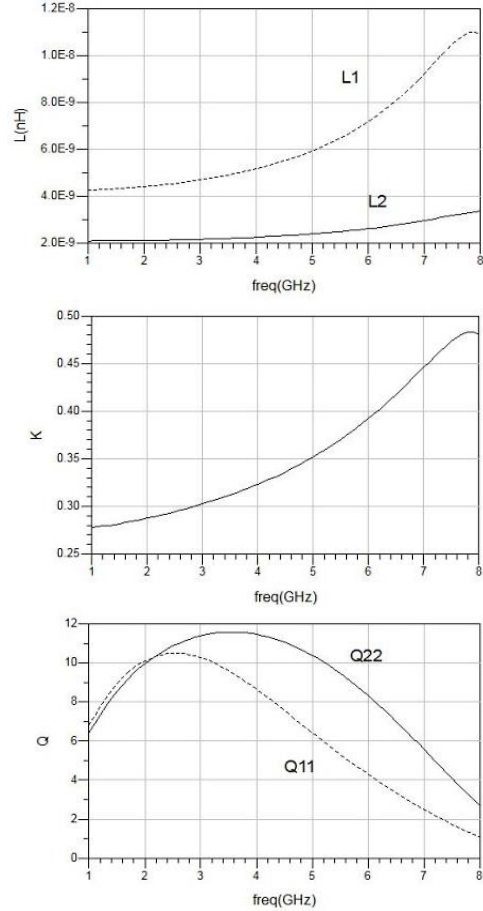Fig. 5. Transformer EM simulation results of VCOH.

Fig. 6. Transformer EM simulation results of VCOL.

III. MEASURENMENT RESULTS

The proposed VCOs are implemented using 0.18μm CMOS technology. Figure 7 shows the micrograph of the VCOs.

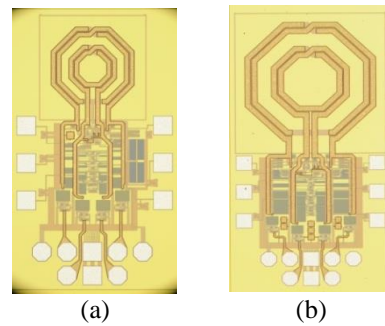Fig. 7. Die micrograph of the proposed VCOs: (a) VCOH and (b) VCOL.

VCOH covers an area of 1084μm×616μm, and VCOL covers an area of 1420μm×710μm. The performances of the fabricated VCOs are evaluated on wafer by

employing a Cascade Microtech probe station. The output spectrum and phase noise of the VCOs are measured by an Agilent E4440A spectrum analyzer.

Figure 8 shows the measured tuning curves of VCOH. The measured phase noise is shown in Fig. 9.
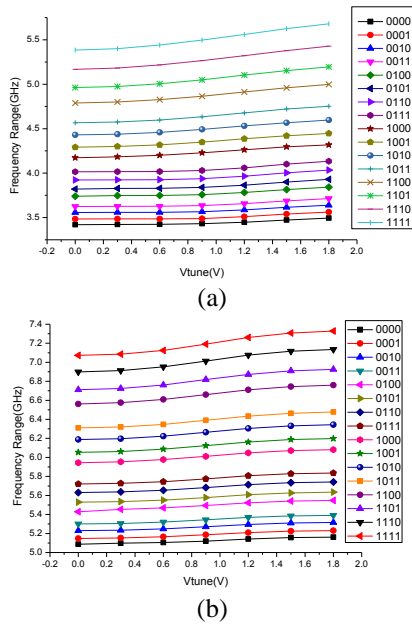

(a)

(b)

Fig. 8. Tuning curves of VCOH: (a) low band in VCOH, and (b) high band in VCOH.
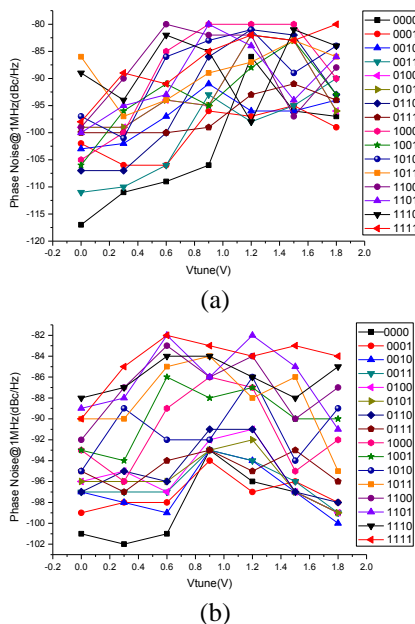

(a)

(b)

Fig. 9. Phase noise@1MHz of VCOH: (a) low band in VCOH, and (b) high band in VCOH.

As the figures show, VCOH is tunable from 3.42 to

5.67 GHz at low band and from 5.12 to 7.33 GHz at high band, resulting in a tuning range of from 3.42 to 7.33 GHz that meets the demand. The phase noise in the whole frequency is less than -80 dBc/Hz but not good enough.

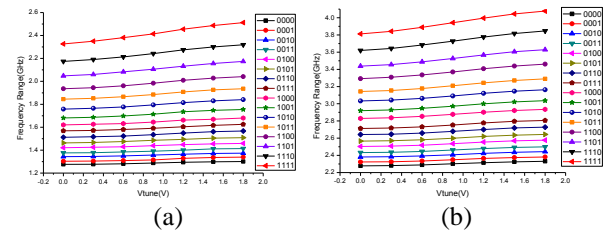Figure10 shows the measured tuning curves of VCOL. The measured phase noise is shown in Fig. 11.

(a)   (b)

Fig. 10. Tuning curves of VCOL: (a) low band in VCOL, and (b) high band in VCOL.

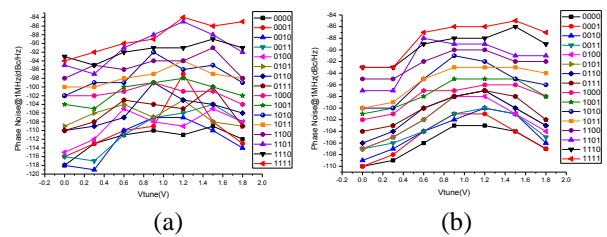

(a)   (b)

Fig. 11. Phase noise @1MHz of VCOL: (a) low band in VCOL, and (b) high band in VCOL.

As the figures show, VCOL is tunable from 1.28 to 2.55 GHz at low band and from 2.29 to 4.03 GHz at high band, resulting in a tuning range of from 1.28 to 4.03 GHz that meets the demand. The phase noise in the whole frequency is less than -84 dBc/Hz.

In Table 1, performance of the present VCO is summarized and compared with recently published dual-band VCOs.

Table 1: Comparison between dual-band VCOs

	Tech. (CMOS)	Supply (V)	Power (mW)	Frequency Range (GHz)	PN (dBc/Hz)
[5]	0.18 μm	1.2	13	0.83-3.72	-104
[7]	0.18 μm	1.0	8	3.4-7.0	-101
[9]	0.18 μm	2.5	15	0.79-0.85 1.75-1.87	-134
[10]	0.18 μm	1.0	10	3.27-5.02 9.48-11.36	-112
This work	0.18 μm	1.8	14.4	3.42-7.3	-84

IV. CONCLUSION

In this paper we use two transformer-based VCOs for the multi-mode multi-standard wireless receivers. The proposed VCOs are fabricated with 0.18μm CMOS technology. Measurement results show that VCOH

exhibits a frequency tuning range of 3.42-7.33 GHz, and the phase noise is less than -80 dBc/Hz at 1 MHz offset from the carrier, VCOL exhibits a frequency tuning range of 1.28-4.03 GHz, and the phase noise is less than -84 dBc/Hz at 1 MHz offset from the carrier.

ACKNOWLEDGMENT

REFERENCES

[1] S. A. Osmany, F. Herzel, and J. C. Scheytt, "An integrated 0.6–4.6 GHz, 5–7 GHz, 10–14 GHz, and 20–28 GHz frequency synthesizer for software-defined radio applications," *IEEE Journal of Solid-State Circuits*, vol. 45, no. 9, pp. 1657-1668, 2010.

[2] J. Kim, J. Shin, S. Kim, and H. Shin, "A wide-band CMOS LC VCO with linearized coarse tuning characteristics," *IEEE Trans. Circuits Syst. II*, vol. 55, no. 5, pp. 399-403, 2008.

[3] W. Zou, X. Chen, K. Dai, and X. Zou, "Switched-inductor VCO based on tapped vertical solenoid inductors," *Electron. Lett.*, vol. 48, no. 9, pp. 509-511, 2008.

[4] Y. Takigawa, H. Ohta, Q. Liu, S. Kurachi, N. Itoh, and T. Yoshimasu, "A 92.6% tuning range VCO utilizing simultaneously controlling of transformers and MOS varactors in 0.13 μm CMOS technology," *IEEE Radio Frequency Integrated Circuits Symp., (RFIC)*, Boston, MA, USA, pp. 83-86, 2009.

[5] J. T. Xu, C. E. Saavedra, and G. Chen, "An active inductor-based VCO with wide tuning range and high DC-to-RF power efficiency," *IEEE Trans. Circuits Syst. II*, vol. 58, no. 8, pp. 462-466, 2011.

[6] M. Demirkan, S. P. Bruss, and R. R. Spencer, "Design of wide tuning-range CMOS VCOs using switched coupled-inductors," *IEEE Journal of Solid-State Circuits*, vol. 43, no. 5, pp. 1156-1163, 2008.

[7] A. Bevilacqua, F. P. Pavan, C. Sandner, A. Gerosa, and A. Neviani, "A 3.4-7 GHz transformer-based dual-mode wideband VCO," *IEEE Eur. Solid-State Circuit Conference.(ESSCRIC)*, pp. 440-443, 2006.

[8] A. Bevilacqua, F. P. Pavan, C. Sandner, A. Gerosa, and A. Neviani, "Transformered-based dual-mode voltage-controlled oscillators," *IEEE Trans. Circuit Syst. II: Express Briefs*, vol. 54, no. 4, pp. 293-297, 2007.

[9] N. Tchamov, S. Broussev, I. Uzunov, and K. K. Rantala, "Dual-band LC VCO architecture with a fourth-order resonator," *IEEE Trans. Circuit Syst. II: Exp. Briefs*, vol. 54, no. 3, pp. 277-281, 2007.

[10] S. Rong and H. C. Luong, "A 1V 4 GHz-and-10 GHz transformer-based dual-band quadrature VCO in 0.18μm CMOS," *Proc. IEEE Custom Integr. Circuit Conference. (CICC)*, vol. 38, no. 8, pp. 1325-1332, 2003.

Xiangning Fan received the B.S. and M.S. degrees both from Nanjing University of Posts and Tele-communications in 1985 and 1988 respectively. From 1997, he became a part time Ph.D. in National Communications Research Laboratory (NCRL), Southeast University and received the Ph.D. degree in 2005 with Grade A.

Since 1988, he works in Southeast University and now he is a Full Professor in Institute of RF-&-OE-ICs, School of Information Science and Engineering, Southeast University. Fan has finished more than 20 national projects on WSN, UWB, and 3G/4G Mobile Systems, and published more than 130 papers in IEEE T-CAS, IEEE COMM. Letters, Signal Processing, IET Radar, Sonar & Navigation, Electronic Letters, Sensor Letters, Springer AICASP, etc. with about 100 papers SCI/Ei indexed. His current research interests include RF ICs, receiver design and signal processing of wireless systems.

Xiaoyang Shi received the B.S. degree in Information Science and Engineering and the M.S. degree in Circuits and System at Southeast University, in 2012 and 2015. His present research interests include frequency synthesizers and RF circuit design.

Li Tang received the B.S. and M.S. degrees in Micro-electronics from Beijing Institute of Technology, China, in 2010 and 2013. He now is currently working towards the Ph.D. degree at Institute of RF-&OE-ICs, Southeast University, China. His research interests include RF integrated circuit design and receiver design.